

See discussions, stats, and author profiles for this publication at: <https://www.researchgate.net/publication/4368591>

IBOAT: An autonomous robot for long-term offshore operation

Conference Paper · June 2008

DOI: 10.1109/MELCON.2008.4618455 · Source: IEEE Xplore

CITATIONS

32

READS

507

1 author:



Yves Briere

Institut Supérieur de l'Aéronautique et de l'Espace (ISAE)

24 PUBLICATIONS 228 CITATIONS

SEE PROFILE

Some of the authors of this publication are also working on these related projects:



Active side-stick [View project](#)

IBOAT: an autonomous robot for long-term offshore operation

Dr Yves Briere
Université de Toulouse, ISAE

Abstract— The concept of autonomous sailing robot is proposed for long term offshore operation as an enhancement for traditional drifting buoys. A prototype of a sailing robot is fully described: structure, sensors, actuators, control system and communication. The sailing boat is modeled and identified from experiments. Control and navigation system is addressed. A simple state machine controller shows very robust performance for both low level and maneuver control.

I. INTRODUCTION

Autonomous sailing robots are relatively new amongst other Autonomous Vehicle like Unmanned Aerial Vehicles (UAV), Underwater Autonomous Vehicles (AUV) and classical terrestrial equivalent robots. The robot we describe in this paper demonstrates that long-term (virtually unlimited) surface navigation can be performed in a fully autonomous way. Ocean observation and monitoring is the main purpose of this kind of robot [1]. Other applications are fish tracking [2], sensor networks for acoustic measurements [3], etc... A sailboat is also a very nice challenge for control: few actuators (only two for our robot), several sensors (only 5 for our robot) and a very unpredictable natural environment: wind, current and sun. Our works are based on a scale 1 prototype in development since 2003 [4], [5]. Geometry, sensors, actuators and systems are roughly the same that will be used on a prototype designed to cross the Atlantic Ocean. The main difference will be mechanical robustness, satellite communication and solar panels (next prototype will have 100 W instead of 20 W of maximum solar power).

This paper address first the design tradeoffs and legal issues. A simulation model is fully derived, control and identification of both simulation model and real robot is explained. The last chapter gives an overview of other similar projects involved in the Microtransat challenge.

II. DESIGN TRADEOFFS

Before launching an unmanned sailing robot at sea, some legal issues must be considered. This problem is regularly addressed in the context of the growing interest for Autonomous Underwater Vehicles ([7]), we give here a quick overview. Although less critical than aerial navigation,

maritime navigation also depends on rules and international conventions. The International Maritime Organization (depending on the United Nation) edited several conventions that are very critical for our unmanned robot. SOLAS 74 stands that "Every vessel must at all times keep a proper look-out". COLREG 72 (and 74-78) is devoted to prevent collisions (lights, flags, maneuvers, etc...) Maneuvers are all based on human operation. SAR 79 (Search and Rescue regulations) says that it is an "obligation for masters to proceed to the assistance of those in distress". Trying to compare our robots to conventional vessels results in complex legal issues ([7]). On the other hand the 1972 International Convention on Ocean Data Acquisition Systems (ODAS) says that these systems must be either tethered to or operated by a conventional vessel and that no particular regulation is needed if the ODAS "does not constitute a potential danger to navigation by reason of its size, material, construction, area or method of operations".

The robot we describe in this paper belongs clearly to the ODAS family: its size (2,4m), weight (35kg) and speed (3knts) cannot reasonably be considered as a potential danger for any other ship.

More generally, length and volume matters in several ways:

- The length of a monohull boat limits its potential speed. The relationship between length L and maximum speed V_{max} is approximately given by the wave propagation speed: $V_{max}(\text{knts}) = 2,43 \times \sqrt{L(\text{meters})}$.

- The volume, Archimedes theorem, is related to the mass of the system. Batteries are the most demanding in term of mass. Clearly, volume is related to autonomy when the energy is totally embedded.

- Between length and volume is the apparent surface of the boat. When covered by solar cell, a 1m^2 surface is able to produce approximately 100W under the better conditions, 10W can be considered as a an average when considering day an night alternance and probability of bad sun coverage.

- Length is also related to mechanical robustness of the sailboat. When dimensioning the mast, sail system, keel and hull one must consider air/boat and water/boat interactions. Water density and air density being in a factor of 1000 the most important effort to take into account is due to water. Our robot being unmanned it is very likely to capsize several times during a long operation. The shortest the mast and keel are, the smallest efforts

This work was supported by ENSICA which is now part of ISAE, Institut Supérieur de l'Aéronautique et de l'Espace, Toulouse, France.

Y. Briere is with ISAE 10 av. Edouard Belin - BP 54032 - 31055, France (e-mail: ybriere@isae.fr).

III. PROTOTYPE

The prototype is made of fiberglass and carbon. The resulting structure is consequently very light. Sail surface has been chosen to be very small: 1,5 m² to be compared to the 4m² expected for this kind of boat. Performance will not be optimal for regular wind but it will be much more robust in case of strong wind. The boat being very light it "lies down" when wind is too strong. Following are the main characteristics of our robot:

TABLE I: IBOAT FACTS

Length	2,4 m
Width	0,4 m
Height	3 m
Weight (including batteries, system, actuators and sensors)	35 kg
Sail surface	1,5 m ²

The sail system is divided in two sails: a main sail and a jib. Only one actuator is needed for the sail since the jib's *tack* is connected to a *balestron*. The whole system rotates thanks to a single actuator (see Figure 1). Another single actuator actuates two rudders. There is no other actuator (like a propeller).

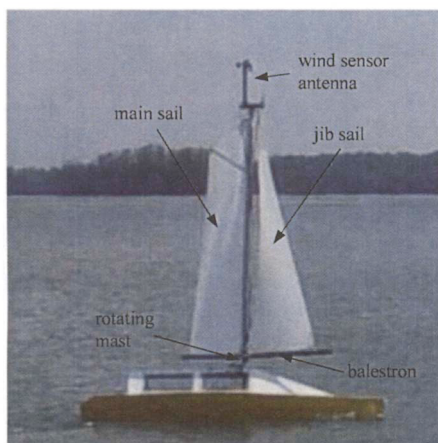


Figure 1 : Photography of the first prototype sailing.

Stepper motors with integrated control are used. They are controlled via a simple CAN protocol (see below).

Sensors are very like the ones used in a real boat. The main sensor is a compass that gives boat's heading: the angle between the longitudinal axis of the boat and the magnetic North. This sensor gives also the rate of turn and roll angle.

A wind sensor is placed on top of the mast (mast orientation is corrected). It gives both speed and heading of the wind. The wind measured is the one experienced by the moving boat: real wind speed and direction is affected by how fast the boat is moving.

The last sensor is a conventional GPS giving position and speed over the ground.

Sensors and actuators are all connected to a microcontroller via a common CAN bus. This bus is very safe and compatible

with the NMEA2000 marine protocol allowing to include commercial marine sensors. The Microcontroller is an Infineon C167 with 2Mb RAM and 2Mb Flash and a 25MHz.clock. In order to optimize computation speed and memory management the embedded code is written in C. The microcontroller main advantage is its power consumption: less than 1W in normal operation. The internal fastest control loop is cadenced at 5Hz and runs the state machine controller (see chapter V.).

An HF radio modem (868 MHz 10km range) is used for ground/sea communication. A serial basic protocol has been designed specifically for this purpose. We currently datalog 100 bytes at a rate of 2Hz. This transmission system is very well fitted for development and research. It will be replaced by a long-range transmission system (satellite) for the long race.

Average power consumption of the whole system (including communication) during a normal sailing test has been measured to be less than 7W.

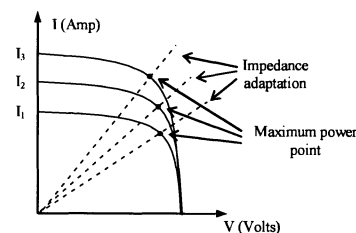


Figure 2 : MPPT principle. Voltage-current characteristics depends on the light (I_0 to I_2 increasing light). The MPPT automatically finds the best power point.

Energy is stored in a classical 14Ah lead battery. Solar photovoltaic cells are used to charge the batteries. The first prototype is equipped with conventional solar panels for a total of only 20 W. This maximum power supposes maximum solar light. Taking into account nights and bad weather probability, we expect a mean of 2 W with this system. Number 2 prototype has integrated solar cells for a maximal amount of 90 W, expecting an average of 10 W. It will be enough for full autonomy of our robot. Interconnection between solar panels and batteries is made via a MPPT (Maximum Power Point Tracking) specially designed system. This system adapts the impedance seen by the solar panels to its maximum power setting (Figure 2). (A survey of different MPPT techniques can be found in [8])

IV. SIMULATION MODEL

Although a first prototype was quite operational we found out that a simulation model was necessary in order to design the control levels. Not many simulation models can be found on the literature for sailing robot. Our model needs to take into account complex behavior (like sailing backward with inappropriate sail tuning!) and a too simple model does not fulfill this requirement. At the other end very accurate models, like in [9], [10] and [11], focus mainly on water/hull interactions and performance prediction (vpp). These models suppose that the sailor constantly optimally tunes sails. An

other drawback is that these models use CFD and are very slow for simulation. We eventually decided to model the sailing boat as a 4 degrees of freedom mobile with simple air/sails and water/hull interactions. Following is a brief description of the model.

A. Inputs, outputs, degrees of freedom, frames

Two frames are used: (XY) denotes the inertial frame (ground) and (xy) the local frame (mobile robot), according to fig 1. Angles are measured clockwise relatively to the North (Y) or longitudinal axis of the boat (y). In the following we use **bold** for vectors.

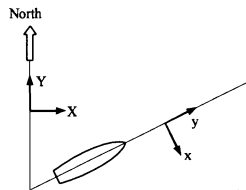


Figure 3 : inertial (XY) and local (xy) frame. (In this figure, the boat is heading +60°)

Inputs are :

- True wind vector **TW**. This is the vector of wind speed relative to the ground.
- True current vector **TC**. This is the vector of the current speed relative to the ground.
- Sail angle **SA**
- Rudder angle **RA**

Outputs are given by the internal sensors :

- True GPS position **XY**
- True GPS velocity **VXY**
- Apparent wind **AW** (velocity and heading). The apparent wind is the wind experienced by the moving robot : $\mathbf{AW} = \mathbf{TW} - \mathbf{VXY}$
- True compass heading **CH**.

Our simulation model has the following four degrees of freedom:

- True Velocity vector of the mobile robot relative to the ground **VXY**. This vector may be expressed into the local frame and is denoted **Vxy**.
- Heading **CH**
- Roll **R**

B. Aerodynamic force

Interactions between sails and wind are responsible for aerodynamic forces and moments. The angle between the apparent wind and the longitudinal axis Oy of the boat is denoted AW (for Apparent Wind). The angle between the sail and Oy is denoted SA (for Sail Angle). The resulting angle of attack is $I = AW + SA$ (I stands for Incidence).

In our model we only consider forces. Moments are supposed to be balanced and the rudder only drives heading of the boat. This hypothesis is well verified by the sea trials, our boat being naturally well balanced.

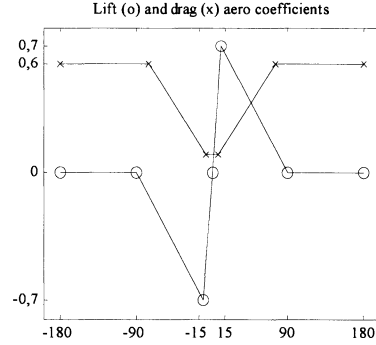


Figure 4 : aerodynamic coefficients (no dimension) versus angle of attack (degrees)

The basics of this very simple aero model are a predefined tabulated lift and drag coefficients curve over a range of 0 to 180 degrees angle of attack (Figure 4).

Lift and drag forces are resulting from the equations:

$$F_{al} = \frac{1}{2} \cdot \rho_a \cdot V^2 \cdot S_a \cdot C_l$$

$$F_{ad} = \frac{1}{2} \cdot \rho_a \cdot V^2 \cdot S_a \cdot C_d$$

Where V is the velocity of apparent wind, ρ_a the relative mass density of air and S the apparent sail surface (see below). The resulting Aerodynamic force is projected along the longitudinal axis Oy and the lateral axis Ox (Figure 5).

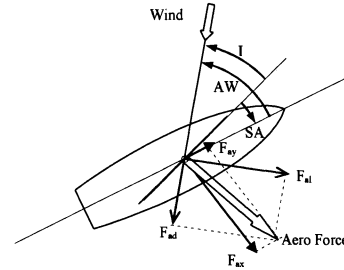


Figure 5 : aerodynamic forces

The apparent sail surface S_a depends on the actual sail surface S and the angle of roll R with:

$$S_a = S \cdot \cos(R)$$

The roll degree of freedom is not properly modeled but a simple relationship has been manually tuned to fit with experiment:

$$R = \frac{K_1}{1 + \tau \cdot s} \cdot \text{atan}(K_2 \cdot F_{ax})$$

(s being the Laplace operator).

C. Hydrodynamic force

Interactions between keel or hull and water are responsible for hydrodynamic forces. Although being a very complex interaction our simple model works fine for our purpose. The hydro model is almost the same than the aero model. The main parameter is now the *leeway* angle L: angle between actual

speed of the boat and the longitudinal axis Oy (Figure 6).

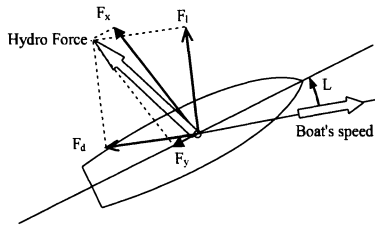


Figure 6 : hydrodynamic forces

Lift force and drag force are computed from a predefined tabulated coefficients curve (Figure 7).

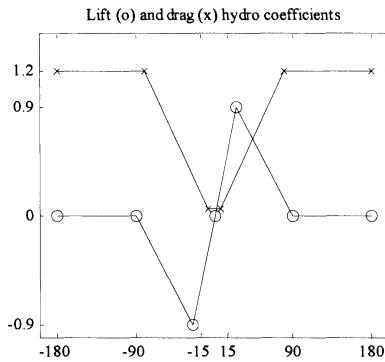


Figure 7 : hydrodynamic coefficients (no dimension) versus angle of drift (degrees)

Lift and drag forces are resulting from the equation:

$$F_{hl} = \frac{1}{2} \cdot \rho_h \cdot V^2 \cdot S_h \cdot C_l$$

$$F_{hd} = \frac{1}{2} \cdot \rho_h \cdot V^2 \cdot S_h \cdot C_{hd}$$

Where V is now the boat's velocity relatively to the surface and S_h the total surface of hull and keel.

Lift and drag force are then projected along Oy and Ox.

D. Longitudinal and lateral dynamics

Longitudinal and lateral aero and hydro forces are simply added resulting in a longitudinal component F_x and a lateral component F_y .

The main hypothesis is now that a virtual mass fully describes the resulting dynamics:

$$V_y = \frac{1}{M_y \cdot s} \cdot F_y$$

$$V_x = \frac{1}{M_x \cdot s} \cdot F_x$$

Like any other, our boat is designed to oppose little resistance along the longitudinal axis: M_y is close to the actual mass of the boat (35kg). The lateral mass has been found to be three times the longitudinal force (100kg).

E. Heading model and dynamics

Aero and hydro forces are considered in our model to be decoupled with heading dynamics. In other terms, hydro and aero moments are neglected. The only force resulting in a rotation along the vertical axis (heading) is generated by the rudder. This is well validated by sea trials: rudder effect is always much stronger than parasite moments.

The chosen model depends on the rudder angle RA, the actual speed V and the sign of the longitudinal component V_y of the boat:

$$\text{Heading} = \frac{1}{s} \cdot K_3 \cdot V^2 \cdot \text{sgn}(V_y) \cdot RA$$

F. Model identification

The main problem for correct parameters identification was the lack of relative speed sensor. Remember that only the GPS speed and course and compass heading are available. The resulting problem is that current speed and course cannot be evaluated directly from our sensors. Following is the relationship between GPS velocity (VXY), velocity relatively to the moving water (V) and the current velocity (GC):

$$VXY = V + TC$$

VXY vector is known from GPS sensor but only argument of V is known from the compass sensor (a speed sensor would give the intensity of V).

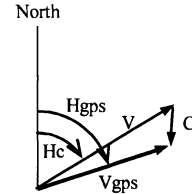


Figure 8 : trajectory against the wind

For a proper identification of dynamic parameters it was necessary to take into account the actual velocity V. V was estimated offline by a conventional mean square estimator. Estimated current was, as expected, not negligible (0.3 kts) compared to the boat's speed (0.5 kts to 3 kts).

A set of sea trials have been conducted in order to identify the parameters. The following table summarizes the numerical values found for each parameter:

TABLE II : IBOAT PARAMETERS

Sail surface (m^2)	S	1,5
Hell and keel surface	S_h	0,2
Longitudinal mass	M_y	35
Lateral mass	M_x	100
Roll coefficient 1	K_1	1
Roll coefficient 2	K_2	0,0051
Heading coefficient	K_3	0.05
Lift and drag aero coefficient	(3 parameters)	(see Figure 4)
Lift and drag hydro coefficient	(3 parameters)	(see Figure 7)

The first three parameters are measured from the actual boat. The other coefficients have been obtained from closed loop experiments ([19]). Figure 9 summarize the procedure for identification of the model M of the system S . The controller C (later described in chapter V. B.) is on the loop for real experiments. Output u_{exp} of the controller, measurements y_{exp} from the system and control input e_{exp} are logged. Classical identification procedure would consist in fitting the model M in order to match the pair $\{u_{exp}, y_{exp}\}$ of Figure 9.1 with the pair $\{u_{exp}, y_{mod}\}$ of Figure 9.2. Our approach consists in taking explicitly into account the controller C during the identification process : the goal was to match the pair $\{e_{exp}, y_{exp}\}$ of Figure 9.1 with the pair $\{e_{exp}, y_{mod}\}$ of Figure 9.3.

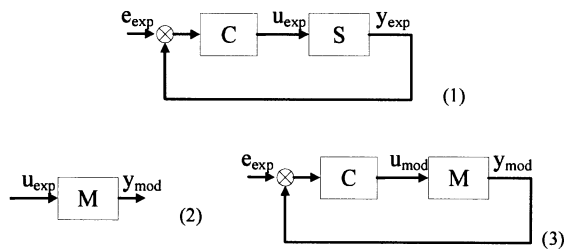


Figure 9 : 1 : closed loop system for experiment ; 2 : open loop modeled system for identification ; 3 : closed loop system for identification.

The main advantage of closed loop identification is that we obtain a very accurate model in the frequency range imposed by the controller C .

Although being very simple our model eventually fits very well the real sea trial. It fits particularly well in case of "tricky" maneuvers:

- backward velocity,
- inappropriate sail tuning,
- side displacements resulting from inappropriate sail tuning.

Last result is the *polar diagram*, obtained from experiment and successfully compared to simulation. For each apparent wind direction and wind force, the maximum speed is obtained by appropriate sail tuning. We obtained the polar diagram depicted in Figure 10

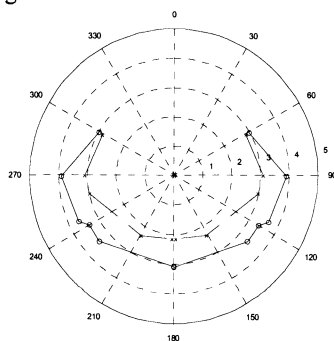


Figure 10 : Polar diagram of the Iboat prototype: velocity (radius) obtained for different apparent wind angle (phase). Diagram obtained for 12knt (solid o) and 9knt (dashed x) wind.

Let us derive a few facts from this diagram. First, it is impossible to sail against the wind (!), secondly the maximum velocity is obtained for wind coming from the rear side (90°), and third there is no significant loss of speed between 90° and 180° .

G. Simulation software

A Matlab/simulink model as been designed according to the theoretical model presented above. The simulation model is enhanced with a sensor and actuators model. It is exactly and fully compatible with the real sailing robot, following the *hardware in the loop* philosophy. The user interface for field tests is consequently also fully compatible with the simulation model.

V. CONTROL AND NAVIGATION

A. Why maneuvering a sailing boat is tricky

Our system looks simple (two inputs: sail and rudder angles and few outputs: compass, GPS, wind sensor) but automatic control is a real challenge. The most important thing is that boat's course cannot face the wind. In other words, the apparent wind angle (the wind experienced by the moving boat) cannot be less than a given angle (55° for our robot).

Sailing at 55° of the apparent wind the boat can maneuver to reach the angle of -55° with a "tacking maneuver". It is done by acting strongly on the rudder.

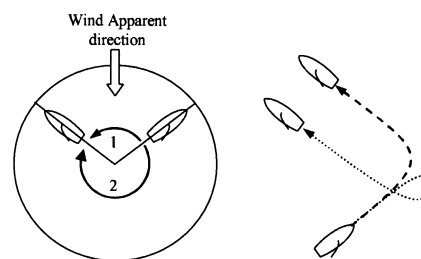


Figure 11 : tacking (1, --) and jibe (2, ..)

Tacking maneuver can fail, mostly when a wind gust occurs at the bad moment. One must first detect this event and either try again to tack or decide to turn in the other direction: this new maneuver (jibe) is safer but the trajectory is not optimal (Figure 11). The resulting trajectory when trying to reach a given point can be a broken line like in Figure 12.

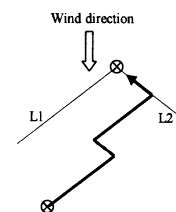


Figure 12 : trajectory against the wind

A basic structure for a sailing boat controller has three levels. Level 1 is the sail and runner low control level

according to the actual desired heading. Level 2 is the maneuver level (mostly tacking and jibe). Level 3 is a strategy level, responsible of the global trajectory (Figure 12) to reach a given waypoint. Lines L1 and L2 are called *laylines*. They show the $\pm 55^\circ$ zone to reach the desired waypoint.

A "natural" approach is to describe sail tuning and rudder control as a set of fuzzy rules and mix everything into a fuzzy controller. Some early examples can be found in the literature [12] [13] for rudder control, and the very last one being a Microtransat competitor [14] for rudder and sail control. Some Neural controller have also been tried ([15] [16]) only for rudder control. Classical high level learning theory has also been applied for the control of a sailboat [17] [18] for rudder control and [6] for rudder and sail control. Only a few real experiments have been conducted so far [12], [14] [1].

B. A simple state machine for control and navigation

The controller we describe here is a very simple state machine and described by only 5 parameters. This controller performs the three levels in a very simple way.

Following is a full description of the algorithm.

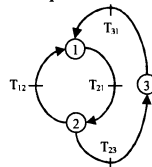


Figure 13 : Sailing state machine

Step 1: compute the desired heading (DH) to reach the waypoint (simple trigonometric calculations from GPS coordinates). The actual heading is denoted H.

Step 2: compare with actual wind heading (WH) and transform the desired heading into a desired relative wind heading (DRWH) and the actual heading into a relative wind heading (RWH) according to :

$$RWH = WH - H$$

$$DRWH = WH - DH$$

Step 3: state machine. The state machine is depicted in Figure 13. The algorithm is described for an initial positive RWH (resp. negative).

There is only three states. State 1 is normal sailing. DRWH is limited to a minimal (resp. maximal) value of $+55^\circ$ (resp. -55°). In case DRWH is less than -30° (resp. more than $+30^\circ$) transition T12 is detected and tacking is ordered: this is state 2. As soon as RWH is below -30° (resp. above $+30^\circ$) T21 is detected and state 1 is active. If T21 is not detected after a timeout of 10s then T23 is detected and state 3 is activated for a jibe. T31 is detected when RWH is below -180° (resp. above $+180^\circ$).

Step 4 : transform DRWH in DH :

$$DH = WH - DRWH$$

Step 5: compute outputs (sail and rudder) according to the

state.

State 1 (normal sailing). The sail is tuned near an optimal angle of attack of 30° with a maximum of 90° according to Figure 14. A hysteresis is added in order to avoid permanent sail tuning and save energy.

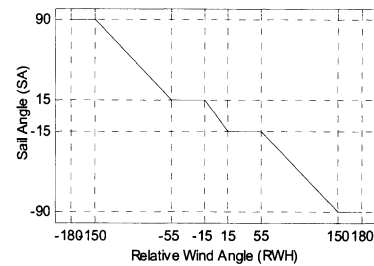


Figure 14 : Optimal sail tuning

Route keeping is realized with a simple proportional controller:

$$RA = k_p \times (DH - H)$$

State 2 (tacking). Tacking maneuver is simply realized by "pushing the rudder" :

$$RA = -80^\circ \text{ (resp. } +80^\circ \text{)}$$

Sail tuning is still done according to Figure 14.

State 3 (jibe) : turn is realized by "pushing the rudder" in the other direction :

$$RA = 80^\circ \text{ (resp. } -80^\circ \text{)}$$

The resulting controller is extremely robust. It takes in charge both the control level and the navigation level. The controller is very simple and needs only 7 parameters.

C. Experimental results

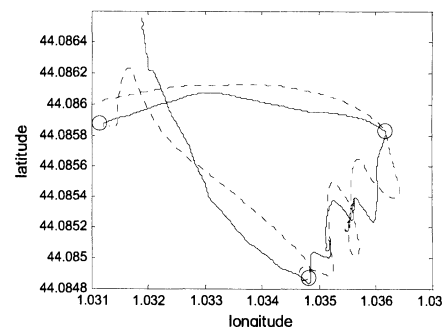


Figure 15 : Simulated (dashed line) versus real (plain line) navigation. Navigation took about 20 mn. Wind average speed is 5 knt, heading mostly West. Estimated current is heading North at 0.2 knt.

The state machine controller has been tested several times in a lake near Toulouse ($44^\circ 05' 09, 21''$ N $1^\circ 01' 51, 32''$ E). As expected from simulation results are very good: the controller takes in charge both control and navigation strategy. Figure 15 shows a navigation between three waypoints (circles). The path is followed clockwise. The plain line is the datalogged navigation path. The dashed line is the simulated navigation while using the recorded wind speed and heading. A higher level controller takes in charge the path planning: when the

distance to a waypoint is less than 5m it is considered to be reached and the goal is the next waypoint in the list.

As seen in Figure 15 the simulation is very close to the actual navigation. Wind measured was heading southwest with a $\pm 40^\circ$ variation and was quite turbulent. Current is heading north and is responsible for the curvature of the first part of the path. There were no significant waves. Some sea trial in more turbulent water has shown the same accuracy. The simulator is very well suited for the design of any kind of closed loop control. Although quite realistic, it is not very accurate for open loop analysis.

VI. THE MICROTRANSAT CHALLENGE

The Microtransat Challenge was initiated by Dr James Mark Neal from the University of Aberswyth (uk) and Dr Yves Briere from ISAE (France). The initial goal was to stimulate the development of autonomous sailing boats through a friendly competition. The first challenge took place near Toulouse in France in 2006¹ with three competitors. The University of Aberswyth in Wales organized the second challenge in 2007² and received four competitors from France, Canada, Austria and Wales. Next step is a challenge in Austria in 2008³. This competition involves small sailing robots (10 to 200kg), autonomy between one hour and 24 hours, and sailing in lakes or near the shore.

The final goal of the Microtransat idea is to demonstrate the ability of long-term operation for autonomous robots using only the power of wind for propulsion. As far as we know three or four teams are close to be ready for the big challenge: crossing the Atlantic Ocean. We can predict that 2008 or 2009 will see the first transatlantic navigation by a fully autonomous sailing robot.

VII. ACKNOWLEDGEMENTS

This work has been supported by ENSICA (Ecole Nationale Supérieure d'Ingénieurs de Constructions Aéronautiques) which is now part of the ISAE (Institut Supérieur de l'Aéronautique et de l'Espace) in Toulouse and IUT of Nantes. Success is widely due to Laurent Alloza (ENSICA) involvement in software and hardware development.

VIII. REFERENCES

- [1] M. Neal, A hardware Proof of Concept of a Sailing Robot for Ocean Observation, IEEE Transaction on Oceanic Engineering
- [2] C. Goudey, T. Consi, J. Manley, M. Graham, B. Donovan, and I Kiley, "A robotic boat for autonomous fish tracking," *Marine technology society journal*, vol. 32, no. 1, 1998.
- [3] B. M. Howe, J. H. Miller, Integrated Acoustics Systems for Ocean Observatories, 3rd International Workshop on Scientific Use of Submarine Cables and Related Technologies, 25-27 June 2003 Komaba Campus, Tokyo, Japan
- [4] Y. Briere, Microtransat project / Iboat website, <http://www.ensica.fr/microtransat/Iboat>

- [5] Y. Briere, F. Bastianelli, M. Gagneul, *Challenge Microtransat*, CETSIS05, Nancy France oct. 25-27 2005
- [6] P. J. Sterne, *Reinforcement sailing*, Master of Science Artificial Intelligence School of Informatics University of Edinburgh 2004
- [7] S. Showalter *The Legal Status of Autonomous Underwater Vehicles*, The Marine Technology Society Journal Spring, 2004; Volume 38, No. 1, pp. 80-83
- [8] T. Esum, P. L. Chapman, *Comparison of Photovoltaic Array Maximum Power Point Tracking Techniques*, IEEE Transactions on Energy Conversion, 2006.
- [9] K. Roncin, J. M. Kobus, *Dynamic simulation of two sailing boats in match racing* Sport Engineering, published in the Sport Engineering Association, vol 7, number 3 2004
- [10] K. Roncin, J. *Simulation dynamique de la dynamique de deux voiliers en interaction* These, Ecole Centrale de Nantes, Juillet 2005
- [11] E. J. Ridder, K. J. Vermeulen, J. A. Keuning, A Mathematical Model for the Tacking Maneuver of a Sailing Yacht, Proc. The International HISWA Symposium on Yacht Design and Yacht Construction 2004
- [12] J. Abril, J. Salom, O. Salom, Fuzzy Control of a Sailboat, *International Journal of Approximate Reasoning* 1997, 16: 359-375, 1995 Elsevier
- [13] E.C. Yeh, J.C. Bin, Fuzzy Control for Self Steering of a Sailboat, *Singapore International Conference on Intelligent Control and Instrumentation*, 1992, Proc. 17-21 Feb 1992, vol2 p1339-1344
- [14] R. Stelzer, T. Pröll, R. I. John, *Fuzzy Logic Control System for Autonomous Sailboats*, in 2007 IEEE International Conference on Fuzzy Systems, London, UK
- [15] F. Fossati, Sailboat Dynamics Identification and Control using Neural Network, *II International Symposium on Yacht Design*, MDY06
- [16] A. Tiano, A. Zirili, C. Yang, C. Xiao, A Neural Autopilot for Sailing Yachts, *9th Mediterranean Conference on Control and Automation*, June 27-29 2001, Croatia
- [17] M.L. van Aartrijk, J. Samoocha, *Learning to Sail* in 'Proceedings of European Symposium on Intelligent Technologies, Hybrid Systems and their implementation on Smart Adaptive Systems (EUNITE 2003), Verlag Mainz, Aachen, 2003
- [18] M. L. van Aartrijk, C. P. Tagliola, and P. W. Adriaans, "AI on the ocean: the robosail project," in Proceedings of European conference on artificial intelligence 2002, 2002, pp. 653-657.
- [19] Landau, Ioan D., Zito, Gianluca, *Digital Control Systems Design, Identification and Implementation* Springer 2006 ISBN: 978-1-84628-055-9



Yves Briere graduated in 1990 from the Institut National Polytechnique de Toulouse, France, with an engineer degree in electrical engineering.

He received a Phd degree in 1994 from the Ecole Nationale Supérieure de l'Aéronautique et de l'Espace (SUPAERO) in automatic control. His initial field of research was force control in teleoperation with time delay.

He was granted by the French government for a Post doctoral fellowship at the robotics laboratory of Stanford, United States, during one year (1994).

After five years at the university of Pau (France) as a professor of electrical engineering he has since 2001 associate professor and researcher at ISAE (ISAE stands for Institut Supérieur de l'Aéronautique et de l'ESPACE) His current field of interest is for control and robotics.

¹ <http://www.ensica.fr/microtransat/Challenge2006/>

² <http://www.microtransat.org>

³ <http://www.roboticsailing.org/en/>